Exploiting oxalotrophic bacteria to control *Aspergillus niger* lung infections

Running title: Bacteria-induced control of aspergillosis

Fabio Palmieri[1], Ilona Palmieri[1], Nourine Noormamode[1], Aislinn Estoppey[1], M. Omar Ishak[2], Julia M. Kelliher[2], Armelle Vallat[3], Rashi Iyer[4], Saskia Bindschedler[1], Karen Davenport[2], Patrick S. G. Chain[2], Jennifer Foster Harris[2], Pilar Junier[1]*.

[1] Laboratory of Microbiology, Institute of Biology, University of Neuchâtel, Neuchâtel, Switzerland.

[2] Bioscience Division, Los Alamos National Laboratory, Los Alamos, NM, USA.

[3] Neuchâtel Platform of Analytical Chemistry, University of Neuchâtel, Neuchâtel, Switzerland

[4] Analytics, Intelligence and Technology Division, Los Alamos National Laboratory, Los Alamos, NM, USA.

*Corresponding author

E-mail: pilar.junier@unine.ch (PJ)

Abstract

The opportunistic pathogen *Aspergillus* affects a record number of people worldwide. Many aspects of the ecology of *Aspergillus* spp. are linked to human pathogenesis, but not their ability to manipulate their environmental pH and enhance infectious potential via the secretion of oxalic acid. Here we showed that co-culturing with bacteria able to degrade oxalic acid (oxalotrophic bacteria) effectively suppress the pH shift induced by *A. niger*, and thereby arrest fungal growth. In 3D-cell culture systems infected with *A. niger*, co-inoculation with as little as 10 cells of an oxalotrophic bacterium was sufficient to return pH, Ca^{2+} and oxalic acid concentrations to the physiological values of uninfected cells. This is the first demonstration of the use of bacteria to control the infection potential of *A. niger*. This approach shifts the focus to the manipulation of the host environment as part of potential interventions to fight opportunistic fungal pathogens.

Introduction

Fungal diseases are estimated to kill more than 1.5 million people every year, with the number of affected patients expected to increase even further (Bongomin et al., 2017; Fisher et al., 2020). Indeed, over the last three decades, the intensification in the burden of fungal disease on human health has correlated with an increase in the number of individuals from at-risk populations (Ramirez-Ortiz and Means, 2012). As the size of these populations (for instance, immunosuppressed patients) is expected to keep increasing in the future (Bongomin et al., 2017), tackling fungal pathogenesis is urgent. However, only a very limited number of antifungal drugs is used nowadays to control fungal pathogens. Because of this restricted chemical arsenal, the same classes of molecules are used in human health, animal husbandry, and agriculture, leading to the rise, and rapid spread, of resistance in fungal pathogens that can

43 affect both plant and animal hosts (Fisher et al., 2018). In spite of this, tackling fungal disease
44 has been largely neglected (Brown et al., 2012).

45 The most prevalent fungal pathogens affecting humans are airborne opportunists such as
46 *Aspergillus* spp., *Cryptococcus* spp., *Pneumocystis* spp., and human-associated commensals
47 like *Candida albicans* (Brunke et al., 2016; Pfaller and Diekema, 2004). These fungal species
48 are responsible for approximately 90% of the deaths due to fungal infection (Fisher et al., 2020).
49 The ecology of all these organisms plays a very significant role in their ability to transition from
50 harmless to pathogenic. A good example of this is the genus *Aspergillus*, whose members are
51 widespread in the environment and are commonly isolated from both the outdoor and indoor
52 environments (Kousha et al., 2011; Paulussen et al., 2017). The remarkable plasticity in the
53 ecology and stress-response of *Aspergillus* spp. is believed to form the basis of its success as
54 an opportunistic pathogen (Paulussen et al., 2017). Indeed, species from this genus, and in
55 particular *Aspergillus fumigatus*, are thought to cause about 450'000 deaths worldwide every
56 year (Brown et al., 2012).

57 Although many aspects of the ecology of *Aspergillus* spp. have been connected to pathogenicity
58 (e.g. nutritional plasticity, reproductive success, and tolerance to environmental stressors), the
59 ability to manipulate pH via the secretion of low molecular weight organic acids, and in
60 particular, oxalic acid, has been largely ignored in the context of human pathogenesis. Several
61 clinical reports have shown the presence of calcium oxalate crystals in pulmonary aspergillosis
62 in animals and humans (Kurrein et al., 1975; Maeno et al., 2015; Muntz, 1999; Oda et al., 2013;
63 Payne et al., 2017; Yi et al., 2019). Oxalic acid and oxalate crystals are thought to directly cause
64 damage to the host tissues (including pulmonary blood vessels), and to generate free radicals
65 which can harm cells indirectly (Payne et al., 2017). A recent case report of invasive pulmonary
66 aspergillosis in a 69-year old man with lymphoma and pneumonia indicated the presence of
67 calcium oxalate crystals around blood vessels and within the blood vessel walls. This suggests

68 a potential mechanical role of oxalate crystals in the angioinvasion of *Aspergillus* (Yi et al.,
69 2019). However, a link between oxalic acid production and pathogenicity has not yet been made
70 in fungi from this genus or in any other fungal human pathogen; despite having been widely
71 acknowledged in the case of fungal plant pathogens, where pH manipulation by the secretion
72 of oxalic acid plays a direct role in pathogenesis (Dutton and Evans, 1996; Lehner et al., 2008;
73 Palmieri et al., 2019). Acidification of the local environment is exploited by plant pathogens to
74 weaken the cell wall structure, facilitate infection, inhibit plant defenses, and induce
75 programmed cell death (de Oliveira Ceita et al., 2007; Dutton and Evans, 1996).

76 Oxalic acid is a ubiquitous compound in the environment. Its production and consumption by
77 microorganisms have been directly associated with pH regulation in soil (Graustein et al.,
78 1977). In such ecosystems, oxalic acid is often found complexed with divalent cations,
79 especially calcium (Martin et al., 2012). Despite its chemical stability (K_{sp} calcium oxalate
80 monohydrate = 2.32×10^{-9}), calcium oxalate rarely accumulates (Certini et al., 2000; Hofmann
81 and Bernasconi, 1998). This is because calcium oxalate is used by soil oxalotrophic bacteria as
82 both a carbon and energy source. The transformation of a strong organic acid into a weaker one
83 (oxalic acid versus carbonic acid; pK_a = 1.25 and 4.14, respectively), creates a local increase in
84 soil pH (Braissant et al., 2004).

85 We hypothesize that oxalic acid production may be needed for *Aspergillus* spp. to manipulate
86 pH during lung infection and that interfering with this process may limit pathogenicity. Such
87 intervention can be accomplished in two different ways. One method is to interfere with the
88 ability of the fungus to produce oxalic acid, for instance by knocking out one or more essential
89 genes in the synthesis pathway. Although valid under laboratory conditions, this option cannot
90 be considered for a therapeutic intervention. The second approach could aim at reducing the
91 concentration of oxalic acid *in situ* by directly removing this compound. This can be achieved
92 by using oxalotrophic bacteria. This approach offers an alternative that can be envisioned for a

93 future therapeutic intervention, based on the manipulation of the lung microbiota (Fig. 1).
94 Therefore, we chose to investigate this second alternative in order to offer a proof-of-concept
95 of the potential of using oxalotrophic bacteria to control the course of fungal pathogenesis.

96 To test our hypothesis, we selected *Aspergillus niger* as a model. This organism has been
97 extensively studied for its ability to produce oxalic acid (Cameselle et al., 1998; Ruijter et al.,
98 1999) and is a known agent of aspergillosis in humans (Paulussen et al., 2017). We first
99 confirmed that *A. niger* secretes oxalic acid and measured the effect of co-cultivation with
100 oxalotrophic bacteria *in vitro*. Then, we investigated the impact of co-cultivation on human
101 bronchial epithelial cells (HBEC) cultures where we determined a dose-response effect for both
102 the fungus and the bacteria. Finally, we used Transwells® inserts and bronchioles-on-a-chip
103 (BoC) systems to measure the effect of the fungus and the co-cultivation with an oxalotrophic
104 bacterium on pH, calcium concentration, oxalic acid concentration, and tissue integrity.

105

106 Results

107 Detection of oxalic acid produced by *Aspergillus niger* in different culture conditions

108 Since the metabolism of fungi can change significantly depending on the nutritional conditions
109 of the growth medium, we first tested whether the strain of *A. niger* used for the experiments
110 produces oxalic acid on different standard laboratory media. Ultra-High Performance Liquid
111 Chromatography (UHPLC) analysis confirmed that the fungus produced oxalic acid as the sole
112 low molecular weight organic acid when grown in malt and in Reasoner's 2 liquid media (Fig.
113 S1A). Acidification and the presence of calcium oxalate crystals could also be detected upon
114 growth in water yeast agar (WYA) (Fig. S1B). We thus concluded that *A. niger* consistently
115 produced oxalic acid and acidified its medium under laboratory growth conditions.

116

117 **Confrontation assays between *A. niger* and selected bacterial strains**

118 We proceeded to test how the presence of oxalotrophic bacteria impacts the growth of *A. niger*
119 and the evolution of the pH in different growth media. Two oxalotrophic bacteria (*Cupriavidus*
120 *necator* and C. *oxalaticus*) and one non-oxalotrophic bacterium (*Pseudomonas putida*) were
121 used in confrontation assays. In malt agar diluted 10 times (MA 1/10), *A. niger* colonized the
122 entire Petri dish, including the area in which the bacterial inocula were applied. All the three
123 bacteria inoculated did not survive in the area of interaction with the fungus (Fig. S2A). In
124 Reasoner's 2 agar (R2A), *A. niger* did not colonize the area beyond the barrier formed by the
125 bacterial inoculum, but some microcolonies formed in the co-culture with *P. putida* beyond the
126 bacterial inoculation zone (Fig. S2B). In water yeast agar (WYA), fungal growth was also
127 restricted to the area delimited by the inocula in the co-culture with the two oxalotrophic
128 bacteria, while *P. putida* did not survive the interaction with the fungus, which instead,
129 colonized the entire plate. Moreover, in WYA medium, which contained a pH indicator, the
130 acidification of the medium by the fungus grown alone or in co-culture with the non-
131 oxalotrophic bacterium was clearly visible. In contrast, in the co-cultures with oxalotrophic
132 bacteria, the pH of the medium did not change (Fig. S2C). The control of fungal growth was
133 particularly remarkable in the case of *C. oxalaticus* (Fig. 2). The results in R2A and WYA
134 validate our hypothesis *in vitro* by demonstrating that fungal growth and pH can be controlled
135 by oxalotrophic bacteria.

136

137 **Growth tests in lung cells culture medium and confrontation assay between *A. niger* and**
138 ***C. oxalaticus***

139 In order to obtain evidence that oxalotrophic bacteria can control the growth of *A. niger* in a
140 lung infection model, we set up experiments on bronchial epithelial cell cultures. Given the
141 impact of the medium on the control of fungal growth, we repeated the growth and
142 confrontation assays in Air-Liquid Interface (ALI) medium, which is the medium used for
143 differentiation of lung cells (Fulcher et al., 2005). The non-oxalotrophic bacterial model (*P.*
144 *putida*) acidified the medium after growth, while the oxalotrophic bacteria (*C. necator* and *C.*
145 *oxalaticus*) did not acidify the medium (Fig S3A). *C. oxalaticus* was found to also inhibit
146 conidia germination and mycelial development (Fig. S3B). Moreover, the presence of *C.*
147 *oxalaticus* in co-culture with the fungus stabilized the pH of the culture medium at a neutral pH
148 (Fig. S3C), consistent with decreased oxalic acid concentration in the medium (Fig. S3D). We
149 therefore conclude that oxalotrophic bacteria have a significant inhibitory effect on *A. niger*
150 growth in ALI medium.

151

152 **Establishment of a dose-response curve on submerged cultures**

153 We established a dose-response curve for increasing conidial and/or bacterial loads on the
154 morphology of HBECs in submerged cultures. This aimed at identifying the optimal conidial
155 and/or bacterial load to perform additional experiments in Transwells® and BoC systems. After
156 24 hours, the overall size, shape and integrity of the lung cells changed at an absolute load of
157 500 conidia and above. The HBECs shrank in size due to actin agglomeration. Moreover, from
158 a conidial load of >=1000, fungal growth also had an adverse effect on tissue integrity (Fig.
159 S4). The same experiment was performed with *C. oxalaticus*. A strong morphological change
160 was induced by a total load of 500 bacterial cells and above. The HBECs became rounder, and
161 actin agglomeration increased compared with the cells-only control (Fig. S5). This indicates
162 that a dose of either 500 conidia or 500 bacterial cells is detrimental. To analyze the effect of

163 co-culturing *A. niger* with the oxalotrophic bacterium on HBECs integrity, we performed a test
164 with 10 and 500 conidia confronted with 10 bacterial cells. After 72h, *A. niger* induced
165 morphological changes (size reduction and actin agglomeration), with a stronger effect for 500
166 conidia, confirming the results obtained in the 24 h experiment. With the co-inoculation of as
167 few as 10 *C. oxalaticus* cells, the morphology of the HBECs was similar to the morphology of
168 HBECs of bacteria-only control, suggesting the inhibition of fungal development (Fig. S6). We
169 concluded that a conidial and bacterial load of 10 conidia/cells was ideal to monitor the
170 interaction of *A. niger* and *C. oxalaticus* in differentiated HBECs in Transwells® and BoC
171 systems.

172

173 **Biocontrol assay of *A. niger* bronchial cells infection by *C. oxalaticus***

174 After establishing a dose-response curve on HBECs in submerged cultures (Fig. S4-S6), the
175 effect of inoculation of 10 conidia of *A. niger* alone or in co-culture with 10 *C. oxalaticus* cells
176 was assessed in differentiated bronchial tissue in Transwells® inserts and BoC systems. In the
177 presence of the fungus alone, changes in three key environmental factors were observed: pH,
178 Ca^{2+} concentration, and concentration of soluble oxalic acid. The pH dropped significantly from
179 7.5 down to 4.5 in Transwells® and from 7.3 to 6.8 in BoC systems (Fig. 3A). Ca^{2+}
180 concentrations changed from 1 mM to around 0.2 mM in both culture systems (Fig. 3B). The
181 level of soluble oxalic acid dropped from 500 µM (cells alone) to 75 µM (cells inoculated with
182 the fungus) (Fig. 3C). pH, Ca^{2+} and free oxalic acid levels were statistically indistinguishable
183 when oxalotrophic bacteria were co-cultured with the fungus or in the controls with cells and
184 bacteria or cells alone. In addition, calcium oxalate crystals were observed in the cultures in
185 which the fungus developed (Fig. 3D), but not when the fungus was co-cultured with
186 oxalotrophic bacteria (Fig. 3E). This suggests that the lower levels of soluble oxalic acid

187 measured in the treatment with the fungus were likely the result of complexation of oxalic acid
188 and Ca^{2+} and corroborates the pH and Ca^{2+} concentration data. Moreover, the absence of
189 calcium oxalate crystals when the fungus was in co-culture with *C. oxalaticus* agrees with the
190 pH, Ca^{2+} concentration and soluble oxalic concentrations measured. These results validated our
191 hypothesis that oxalotrophic bacteria can be used to manipulate the microenvironment created
192 by *A. niger* and to hamper its development.

193 In addition to the changes in the environmental parameters measured above, we also observed
194 a cytopathic effect when conidia of *A. niger* developed into mycelia (Fig. 4A and B). The
195 absence of lactate dehydrogenase (LDH) activity measured in the medium in the treatment with
196 *A. niger* (Fig. 4C), supports the cytopathic effect and aggressiveness observed upon infection
197 by *A. niger*. LDH measurements were elevated in response to the presence of oxalotrophic
198 bacteria. Indeed, *C. oxalaticus* is a soil bacterium that is completely foreign to the lung
199 environment, thus potentially inducing an inflammatory response, something that needs to be
200 addressed for any future therapeutic application.

201

202 Discussion

203 By demonstrating the biocontrol activity that oxalotrophic bacteria exerted on *A. niger*, our
204 study represents a novel paradigm in which the manipulation of the lung environment can
205 become the focus of an anti-fungal medical intervention. This contrasts with the prevailing use
206 (and abuse) of antimicrobial compounds, which are instead directed to the pathogen and
207 inevitably result in the emergence of resistance (Toprak et al., 2011). To our knowledge, this is
208 the first demonstration of such an alternative approach for combatting human fungal infections
209 and is a significant step towards an integrated disease management strategy that is urgently
210 required to slow the emergence of resistance in fungal pathogens. Moreover, this approach can

211 be also relevant to *A. fumigatus*, the major causative agent of pulmonary aspergillosis, as the
212 presence of calcium oxalate crystals has been reported in the literature, suggesting also the
213 production of oxalic acid production by this pathogen (Kousha et al., 2011; Maeno et al., 2015;
214 Pabuççuoğlu, 2005; Payne et al., 2017). Currently there is an increasing interest in applying
215 ecological theory in lung microbiome research (Foesel et al., 2019). Although considered sterile
216 for a long time, the lung is now known to harbor a diverse microbiota (Enaud et al., 2020;
217 Mitchell et al., 2016). In the healthy lung, this microbiota is dominated by the genera *Prevotella*,
218 *Streptococcus* and *Veillonella* (Charlson et al., 2011; Foesel et al., 2019). Its composition differs
219 in a diseased state (Cui et al., 2015; Dickson et al., 2014; van Woerden et al., 2013) and after
220 transplantation (Charlson et al., 2012). This dysbiosis of the lung microbiota, which can be
221 associated with comorbidities in at-risk patients, could make the lung environment more
222 permissive to fungal pathogens such as *Aspergillus* spp. This could in part explain the current
223 epidemic of nosocomial fungal infections (Suleyman and Alangaden, 2016).

224 Oxalate-degrading capabilities have been previously reported in strains of the genera
225 *Lactobacillus* (Turroni et al., 2007), *Streptococcus* (Miller and Dearing, 2013), *Prevotella*
226 (Suryavanshi et al., 2016; Ticinesi et al., 2020) and *Veillonella* (Suryavanshi et al., 2016), all
227 of which are represented in the lung microbiota. In this context, assessing the oxalotrophic
228 potential of the lung microbiome and its subsequent stimulation could offer an endogenous
229 alternative to fight aspergillosis. Indeed, as aspergillosis mainly affects immunocompromised
230 patients, the administration of an exogenous bacterial species as therapeutic intervention could
231 be unviable. Nevertheless, complementing the microbiota with a specific bacterial strain, or
232 even a consortium, has been proven successful in protecting the host from *Clostridium difficile*
233 infection in a mouse model (Buffie et al., 2015; Lawley et al., 2012). Another potential venue
234 is the administration of a completely abiotic delivery system of oxalate-degrading enzymes
235 directly in the lungs by inhalation.

236 Our results also provide an indication of potential additional roles of oxalic acid in fungal
237 pathogenesis in humans. Secretion of oxalic acid by the fungus has a clear effect on the
238 concentration of free Ca^{2+} in the medium. Calcium is known to be a secondary messenger in
239 many cell types, playing a central role in the activation of the immune response (Vig and Kinet,
240 2009). During immune stimulation, the concentration of intracellular Ca^{2+} in immune cells
241 increases thanks to Ca^{2+} entry from the extracellular media or cellular compartments (Grinstein
242 and Klip, 1989). Accordingly, the use of a chelating agent of divalent cations has been shown
243 to inhibit the immune response *in vitro* (Diamantstein and Odenwald, 1974; Diamantstein and
244 Ulmer, 1975). This suggests that chelation of Ca^{2+} in calcium oxalate crystals upon fungal
245 infection could inhibit the immune response. Moreover, the detection of calcium oxalate
246 crystals is also meaningful in the case of a chronic inflammatory response, as calcium oxalate
247 crystals have been involved in inflammation in renal cells (Mulay et al., 2013). A recent study
248 also shows that calcium oxalate crystals induce the production of inflammatory cytokines in
249 primary and THP-1 monocytes (Dominguez-Gutierrez et al., 2018). Finally, a recent study from
250 McClintock *et al.* (McClintock et al., 2020) showed the role of calcium in epithelial tissue
251 cohesion and barrier function, which could be disrupted upon fungal infection and subsequent
252 Ca^{2+} sequestration in the form of calcium oxalate.

253 The results presented here are the stepping-stones for the development of a pre-clinical *in vivo*
254 animal model and the subsequent validation of the proposed approach in order to translate these
255 results into a potential clinical application. Indeed, a more holistic approach with the integration
256 of the immune system components will be key to understand the interplay between the host, the
257 lung microbiota, the environment, and the pathogen.

258

259

260 ## Materials and Methods

261 ### Bacterial and Fungal cultures

262 All bacterial and fungal strains used in this study come from the collection of the Laboratory
263 of Microbiology of the University of Neuchâtel (LAMUN) and are summarized in Table 1. *P.*
264 *putida* KT2440 was kindly provided by Dr. Arnaud Dechesne (Technical University of
265 Denmark). *C. necator* JMP289 was kindly provided by Prof. Jan van der Meer (University of
266 Lausanne). *C. oxalaticus* Ox1 was tagged in-house using insertion with a MiniTn7 system.
267 Bacterial strains were routinely cultured on Nutrient Agar (NA, Carl Roth, Karlsruhe,
268 Germany) medium, whereas *Aspergillus niger* was routinely cultured on Malt Agar (MA)
269 medium. Potato Dextrose Agar (PDA, Carl Roth, Karlsruhe, Germany) was used for *A. niger*
270 conidia production. MA medium was composed of 12 g/L malt extract (Sios Homebrewing
271 GmbH, Wald, Switzerland) and 15 g/L agar (Biolife Italiana, Milano, Italy). Brain Heart
272 Infusion Agar (BHIA, Brain Heart Broth, Sigma-Aldrich, Darmstadt, Germany, 15 g/L agar)
273 was used to have mycelium-only colony edge without any conidia.

274

275 **Table 1. Bacterial and fungal strains used**

Code	Strain #	Species	Fluorescent tag	References
Pp	NEU 1264	*Pseudomonas putida* KT2440	GFP	
Cn	NEU 1286	*Cupriavidus necator* JMP289	GFP	(Sentchilo et al., 2009)
Co	NEU 1287	*Cupriavidus oxalaticus* Ox1	mCherry	(Şahin et al., 2000)

An	NEU M8	*Aspergillus niger*	-	(Ferro, 2012)

All the bacterial and fungal strains used in this study come from the collection of the Laboratory of Microbiology of the University of Neuchâtel.

Low Molecular Weight Organic Acids (LMWOA) detection by UHPLC and by colorimetric pH indicator-based Petri dish assay

In order to highlight the production of LMWOA by *A. niger*, we used Ultra-High-Performance Liquid Chromatography (UHPLC), as well as a culture-based assay by using a pH indicator-containing agar culture medium.

For the UHPLC analysis, 500 µl of 30 mM H_2SO_4 were added to 1 mL of a two-week liquid culture in malt 1/10 and Reasoner's 2 liquid media in triplicate, to obtain 20 mM H_2SO_4 final concentration. The samples were incubated at 60°C for two hours in order to dissolve precipitated metal oxalate crystals, and then centrifuged at 3000 g for 10 min. All the samples were filtered at 0.22 µm (13mm syringe filters, PTFE, hydrophilic) and 200 µl were added into HPLC vials with 250 µl conical inserts. UHPLC (Ultimate 3000 RS-Dionex, Thermo Fisher Scientific, MA, USA) was coupled with DAD detector set at 210 ± 2 nm. A 5 µL of sample was injected onto a Prevail^{TM} organic acid column (5 µm particle size, 150 x 4.6 mm, Grace Davison Discovery Sciences, Deerfield, IL, USA) with the temperature kept at 40°C. The mobile phase consisted of 50 mM phosphate buffer adjusted to pH 2.5 with phosphoric acid with a flow rate of 1 mL/min. Pure oxalic acid (Merck KGaA, Darmstadt, Germany) was identified by the retention time and was quantified by an external standard curve, linear regression from five calibration points (0.2 to 5 mg/mL).

297 For the culture-based assay, water yeast agar supplemented with bromocresol purple
298 (WYA+BP) (Mela et al., 2011) was used as a pH indicator-containing medium. WYP+BP was
299 composed of 1 g K_2HPO_4, 5 g NaCl, 0.1 g yeast extract, 10 mg bromocresol purple and 20 g
300 agar, per liter of Milli-Q® water. After one week of incubation at room temperature, the
301 presence of typical bi-pyramidal shaped calcium oxalate crystals was assessed by observing a
302 thin slice of agar medium sampled at the edge of the colony and stained with lactophenol cotton
303 blue under a Leica DM4 B optical microscope connected to a Leica DFC7000 T camera.

304

305 **Confrontation assays on solid media**

306 Confrontations assays were performed between *A. niger* and three bacterial strains:
307 *Pseudomonas putida*, *Cupriavidus necator* and *Cupriavidus oxalaticus*, on three culture media
308 differing in their nutrient content. Malt agar diluted ten times (MA 1/10) was used as nutrient-
309 rich medium and was composed of 1.2 g/L malt extract (Sios Homebrewing GmbH, Wald,
310 Switzerland) and 15 g/L (Biolife Italiana, Milano, Italy). Reasoner's 2 agar (R2A) (Reasoner
311 and Geldreich, 1985) was used as nutrient-poor medium and the composition per liter of Milli-
312 Q® water was the following: 0.5 g yeast extract, 0.5 g Bacto Peptone, 0.5 g casamino acids,
313 0.5 g glucose, 0.5 g soluble starch, 0.3 g Na-pyruvate, 0.3 g K_2HPO_4, 0.05 g $MgSO_4 \cdot 7H_2O$
314 and 15 g agar. WYA+BP (Mela et al., 2011) was also used. *A. niger* was inoculated in the center
315 of the plates containing the different culture media. For that, a plug coming from the apical part
316 of an active colony was sampled using the wider end of a Pasteur pipette. The three different
317 bacterial strains were inoculated as opposite lines on either side of the fungal inoculum. Plates
318 were incubated at room temperature for 20 days, and pictures of the plates were taken. Pictures
319 of the bacterial inocula were taken using a Nikon SMZ18 epifluorescence stereoscope,

320 connected to a Nikon DS-Ri2 camera, in order to assess the viability of the bacterial strains
321 thanks to constitutively expressed fluorescent proteins.

322

323 **Growth tests and confrontation assay in Air-Liquid Interface (ALI) medium**

324 Air-Liquid Interface (ALI) medium was composed of DMEM/F12 (Cat.# 11320033, Thermo
325 Fisher Scientific) and LHC Basal Medium (Cat.# 12677019, Thermo Fisher Scientific) at a 1:1
326 ratio according to Fulcher *et al.* (Fulcher et al., 2005). Bacterial growth in ALI medium was
327 tested for 3 days at room temperature. Increasing concentrations of Ca^{2+}, from 1 mM to 10 mM,
328 was also tested on bacterial and fungal growth in a 96-well plate. Given that ALI medium
329 contains 1 mM Ca^{2+}, a 10 mM Ca^{2+} stock solution of ALI medium was prepared by adding 1.32
330 g/L $CaCl_2$ to have an added Ca^{2+} concentration of 9 mM. This stock solution was used to prepare
331 8, 7.5, 6, 4.5, 3, and 2.5 mM dilutions of $CaCl_2$ ALI-containing media. To produce fungal
332 conidia, *A. niger* was cultured on PDA for 10 days at room temperature. Conidia were then
333 harvested by using Dulbecco's Phosphate Buffer Saline (DPBS) supplemented with 0.01%
334 (v/v) Tween 80. Harvested conidia were washed tree times with DPBS following centrifugation
335 at 2000xg for 5 min at room temperature. Finally, conidia were resuspended in 2 mL DPBS and
336 quantified with an Improved Neubauer counting chamber. Two µL of 16'000 conidia/bacterial
337 cell per µL suspensions were inoculated in 200 µL ALI medium containing the Ca^{2+}
338 concentrations indicated above. To test mycelial growth in the different media, small agar plugs
339 (approximately 3 x 3 mm) coming from the edge of a colony of *A. niger* on BHIA were used.
340 The 96-well plate was incubated at room temperature for 7 days and growth was visually
341 assessed.

342 Confrontation of *A. niger* with *C. oxalaticus* was performed in 100-mm Corning® tissue culture
343 plate containing 12 mL ALI medium to allow the fungus to attach during growth. The fungal

344 inoculum was taken from the apical part of an active colony grown on BHIA by using the wider
345 end of a Pasteur pipette. For the confrontation assay, the fungal inoculum was placed in the
346 medium after addition and mixing of 100 µL inoculum of an overnight culture of *C. oxalaticus*
347 in ALI medium. A fungus-only plate was used as control. The plates were incubated at room
348 temperature for 7 days. Oxalic acid concentration was quantified by using the Oxalic Acid
349 Colorimetric Assay Kit (Sigma-Aldrich, Darmstadt, Germany, Cat.# MAK179), following the
350 manufacturer instructions.

351

352 **Preparation and sterilization of the bronchiole-on-a-chip (BoC)**

353 The chip was assembled as described in Hsieh, Nath and Huang (Hsieh et al., 2019). Each unit
354 of the culture platform was fabricated by using a layer-by-layer stacking technique (Lin et al.,
355 2019). The devices were designed using Solid Edge 2D software (ST9, Siemens PLM
356 Software), and each layer of the prelaminated polymeric sheet was obtained using a CO_2 laser
357 cutter (Universal Laser System). The prelaminated polymeric sheets were combined with
358 biocompatible adhesive tapes (9122, 3M Company) with PMMA (1.5 and 3 mm thick) or PET
359 (0.1 and 0.25mm thick). After cutting, each layer was aligned and assembled using a seam roller
360 to complete the devices. The culture chip includes a Y-shaped apical and a basal part separated
361 by a porous PET membrane (pore size = 0.4µm) prepared as described in Arefin *et al.* (Arefin
362 et al., 2018). The PET membrane was sandwiched between two PET sheets using adhesive
363 transfer tape to create the cell culture surface. This allows nutrients to pass from the media to
364 the cells through the porous membrane. The open design of the tissue chip makes cell seeding
365 procedure easy and accessible.

366 For sterilization, each chip was placed in a 100 mm Petri dish and sterilized with 5% hydrogen
367 peroxide solution for one hour. The chips were then rinsed 2-3 times with sterile deionized

368 water for 15 min between each rinse. Once all liquid was removed, the chips were let dry
369 overnight under a laminar flow hood. The next day, the inlet and outlet of the chip were
370 connected with a sterile tubing and rinsed 3 more times with sterile deionized water as explained
371 before. After the last rinse, 200 µl sterile DPBS was added in the channel (apical part) and 5
372 mL in the basolateral part (bottom part) of the chip, and the chip was placed in a humidified
373 incubator at 37°C with 5% CO_2 overnight. The next morning, peroxide contamination was
374 checked in each chip using a CG8+ i-STAT cartridge (Abbott, USA, Cat.# 03P88-25). Rinses
375 with sterile deionized water and overnight incubation with sterile DPBS were repeated until
376 peroxide was no longer detected in the devices.

377

378 **Primary normal human bronchial epithelial cell culture**

379 Primary normal human bronchial epithelial cells (Lifeline Cell Technology, Cat.# FC-0035)
380 were expanded in a T-75 cell culture flask with vent cap (Corning, Cat.# 3290) containing 13
381 mL BronchiaLife™ B/T complete medium (Lifeline Cell Technology, Cat.# LL-0023)
382 supplemented with 3 mL/L 0.5% Phenol Red solution (Sigma-Aldrich, Cat.# P0290, 15 mg/L
383 final concentration) to 70-80% confluence in a humidified incubator at 37°C with 5% CO_2.
384 Culture medium was changed every other day. Cells were used until passage 2 maximum for
385 all experiments. Cells were then harvested by trypsinization with 0.05% Trypsin / 0.02% EDTA
386 (Lifeline Cell Technology, Cat.# CM-0017), followed by the addition of Trypsin Neutralizing
387 buffer (Lifeline Cell Technology, Cat.# CM-0018), and counted using a hemocytometer after
388 centrifugation at 100xg for 5 min and resuspension of the cell pellet in BronchiaLife™ medium.

389 For submerged undifferentiated tissue culture in 96-well plates, 30’000 cells were seeded in
390 200 µl BronchiaLife™ medium per well. The 96-well plate was placed in a humidified

391 incubator at 37°C with 5% CO_2 for 2-3 days until confluence and formation of a monolayer of
392 bronchial cells.

393 For air-lifted differentiated tissue culture, Transwell® inserts in 24-well plates (Corning, Cat.#
394 3470) and BoC devices have first to be coated with collagen in order to allow proper cell
395 attachment onto the porous membrane. For that, 200 µL of 30 µg/mL rat collagen (Corning,
396 Cat.# 354236) diluted in DPBS were added to the apical side of Transwell® inserts and BoC
397 devices and the latter have been placed at 37 °C for 4 h in a 5% CO_2 humidified incubator.
398 Excess collagen was then removed, and all inserts and devices were rinsed once with sterile
399 DPBS and stored in a refrigerator until seeding of the cells.

400 Transwell® inserts and BoC devices were seeded on the apical side with 50'000 cells and
401 86'000 cells in 200 µL BronchiaLife™ complete medium, respectively. 600 µL of
402 BronchiaLife™ complete medium was added to the basolateral side of Transwell® inserts in
403 the 24-well plates and 3 mL in the basolateral side of the BoC device. All the inserts and device
404 were then placed in a humidified incubator at 37°C with 5% CO_2 for 2-3 days until confluence.
405 When bronchial cells formed a monolayer, they were shifted to air-liquid interface.
406 BronchiaLife™ complete medium was removed carefully from the apical part and replaced by
407 Air-Liquid Interface (ALI) Epithelial Differentiation Medium (Lifeline Cell Technology, Cat.#
408 LM-0050) supplemented with 3 mL/L 0.5% Phenol Red solution (Sigma-Aldrich, Cat.# P0290,
409 15 mg/L final concentration). The same was done for the medium in the basolateral side.
410 Finally, the medium on the apical side was removed and the inserts and devices were placed in
411 a humidified incubator at 37°C with 5% CO_2 for 21 days. Medium was changed every other
412 day as described previously. The cultures were observed daily using an EVOS™ XL Core
413 bright field inverted microscope (Thermo Fisher Scientific, CA, USA).

414

415 **Determination of conidial and bacterial load and confrontation assay on submerged**
416 **undifferentiated bronchial epithelial cell cultures**

417 In order to determine the optimal conidial and bacterial load to be used for confrontation on
418 bronchial tissue cultures, increasing conidial and bacterial loads were tested to assess their
419 effect on the morphology of bronchial epithelial cells in submerged cultures. *A. niger* was
420 cultured on PDA for 7 days at 37°C in order to produce conidia. *A. niger* conidia were then
421 harvested as already described. Finally, conidia were resuspended in 2 mL DPBS and quantified
422 with an Improved Neubauer counting chamber. Bacteria were cultured in BronchiaLife™
423 complete medium at 37°C overnight and quantified with an Improved Neubauer counting
424 chamber. A stock suspension of *A. niger* conidia was made at 1'000'000 conidia/mL that was
425 diluted further to obtain suspensions at 500'000, 100'000, 50'000, 10'000, 5000 and 1000
426 conidia/mL. The same was done for *C. oxalaticus* from a stock suspension at 100'000 bacterial
427 cells/mL diluted until 1000 bacterial cells/mL. 10 µL of each suspension was added to
428 submerged undifferentiated bronchial tissue in a 96-well plate in order to have 10'000, 5000,
429 1000, 500, 100, 50 and 10 conidia/well (200 µL) for *A. niger*, and 1000, 500, 100, 50, 10
430 bacterial cells/well (200 µL) for *C. oxalaticus*. The plates were placed in a humidified incubator
431 at 37°C with 5% CO_2 for 24h. For the confrontations assay, cells were infected with 10 or 500
432 *A. niger* conidia and were put in confrontation with 10 bacterial cells. Controls with only cells,
433 fungus or bacteria were also prepared. The plate was placed in a humidified incubator at 37°C
434 with 5% CO_2 for 72h.

435 After 24h or 72h incubation, the cells were fixed by adding 100 µL 4% paraformaldehyde in
436 DPBS per well and the plates were let sit for 15 min at room temperature. The cells were then
437 rinsed 3 times, with 2 min waiting time between each rinse. Two drops of ActinGreen™ 488
438 ReadyProbes™ Reagent (actin stain, Thermo Fisher Scientific, Cat.# R37110) and one drop of
439 NucBlue™ Live ReadyProbes™ Reagent (nuclei counterstain, Thermo Fisher Scientific, Cat.

440 # R37605) was added in 1 mL of DPBS to prepare the staining solution. 200 µL of staining
441 solution were added per well and the plates were let sit for 30 min at room temperature. Finally,
442 the cells were washed 3 times with DPBS before imaging with a Zeiss Axio Observer Z1
443 fluorescence inverted microscope (Carl Zeiss AG, Oberkochen, Germany).

444

445 **Confrontations on differentiated bronchial tissues in Transwell® inserts and BoC devices**

446 Differentiated bronchial tissues in Transwell® inserts and in BoC devices were infected with
447 10 µL of 1000 conidia or bacterial cell to get 10 conidia or bacterial cells. Fungus and bacteria
448 were co-inoculated for the confrontation and controls with only medium, cells, fungus or
449 bacteria were included. Each condition was done in triplicate for the Transwell® inserts and
450 one unique replicate for each condition was done for the BoC devices. All Transwell® inserts
451 and BoC devices were incubated in a humidified incubator at 37°C with 5% CO_2 for 72h.

452

453 **Immunofluorescence staining**

454 Differentiated bronchial tissues in Transwell® inserts and BoC devices were fixed by adding
455 100 µL 4% paraformaldehyde in DPBS per insert or device and the 24-well plate and devices
456 were let sit for 15 min at room temperature. The cells were then rinsed 3 times with 200 µL
457 DPBS, with 2 min waiting time between each rinse. Cells were permeabilized with 100 µL
458 0.5% Triton X-100 in DPBS for 15 min at room temperature and rinsed 3 times with 200 µL
459 DPBS, with 2 min waiting time between each rinse. After that, cells were blocked with 100 µL
460 3% BSA in DPBS for 1h at room temperature. Anti-Mucin 5AC mouse monoclonal antibody
461 (Abcam, Cat.# ab218466) was prepared in DPBS (1/100). The actin stain (ActinGreen™ 488
462 ReadyProbes™ Reagent, Thermo Fisher Scientific, Cat.# R37110) and the nuclei counterstain
463 (NucBlue™ Live ReadyProbes™ Reagent, Thermo Fisher Scientific, Cat. # R37605) were

464 added to the same buffer (2 drops/mL and 1 drop/mL, respectively). Anti-Aspergillus rabbit
465 polyclonal antibody (Abcam, Cat.# ab20419, RRID:AB_445571) was also added (1/200) in the
466 staining buffer for the conditions where *A. niger* conidia were inoculated. Fixed cells were
467 incubated with 100 µL buffer containing the stains and Anti-Mucin 5AC and Anti-Aspergillus
468 antibodies overnight at 4°C. The next day, fixed cells were washed 3 times with DPBS and
469 secondary antibodies were applied. Goat anti-Mouse IgG antibody (1/250) conjugated with
470 Alexa Fluor 546 (Thermo Fisher Scientific, Cat.# A-11003, RRID:AB_2534071) directed
471 against Anti-Mucin 5AC antibody and Goat anti-Rabbit IgG antibody (1/500) conjugated with
472 Alexa Fluor 594 (Thermo Fisher Scientific, Cat.# A-11012, RRID:AB_2534079) directed
473 against Anti-Aspergillus antibody were prepared in DPBS. Fixed cells were incubated with 100
474 µL buffer containing the secondary antibodies overnight at 4°C. The following day, fixed cells
475 were once again washed 3 times with DPBS and the membranes from the inserts were carefully
476 cut out with a sharp knife. The membranes were mounted on a glass slide using Fluoromount-
477 G™ Mounting Medium (Thermo Fisher Scientific, Cat.# 00-4958-02) and imaged with a Zeiss
478 Axio Observer Z1 fluorescence inverted microscope (Carl Zeiss AG, Oberkochen, Germany).

479

480 **pH measurements and quantification of calcium, oxalic acid and lactate dehydrogenase**
481 **(LDH)**

482 pH measurements of the culture medium after 72h incubation were done directly after taking
483 the samples out of the incubator using pH-indicator strips (Merck, Germany, Cat.# 109535) for
484 the Transwell® inserts samples, and CG8+ i-STAT cartridges (Abbott, USA, Cat.# 03P88-25)
485 for the BoC devices, as the pH change of the culture medium indicator was less visible. Free
486 calcium (Calcium Colorimetric Assay, Sigma-Aldrich, Darmstadt, Germany, Cat.# MAK022),
487 free oxalic acid (Oxalic Acid Colorimetric Assay Kit, Sigma-Aldrich, Darmstadt, Germany,

488 Cat.# MAK179), and LDH (ScienCell Research Laboratories, CA, USA, Cat. # 8078) were
489 quantified in the culture medium using colorimetric assay kits following the manufacturer
490 instructions.

491

492 **Statistical analyses**

493 Statistical significance of the data from the confrontations on differentiated bronchial tissues in
494 Transwell® inserts (3 replicates, n = 3) was tested with unpaired two-tailed Student t-tests in
495 Microsoft® Excel (Version 16.37). The statistical significance threshold was set to 5%.

Acknowledgments

We would like to thank Diego Gonzales and Ted Turlings for critical review of the paper, and Pulak Nath from the Materials Physics and Applications Division of the Los Alamos National Laboratory for providing the equipment and laboratory infrastructure for the BoC devices fabrication. BoC devices were developed under Defense Threat Reduction Agency (DTRA) interagency agreement CBMXCEL-XL1-2-0001. **Author contributions:** FP, PSC, JFH and PJ conceived and designed the study. FP, IP and NN performed the *in-vitro* experiments. AV performed the UHPLC analysis. FP performed the experiments related to cell work. JMK performed the microscopic observation of the CaOx crystals in the differentiated bronchial epithelial tissue. MOI fabricated and assembled the BoC devices. FP, JFH and PJ analyzed the data. FP and PJ wrote the paper, and all the authors reviewed and edited the paper. **Data and materials availability:** All data is available in the main text or the supplementary materials. **Competing interests:** Authors declare no competing interests.

510 **References**

511 Arefin A, McCulloch Q, Martinez R, Martin SA, Singh R, Ishak OM, Higgins EM, Haffey
512 KE, Huang J-H, Iyer S, Nath P, Iyer R, Harris JF. 2018. Micromachining of Polyurethane
513 Membranes for Tissue Engineering Applications. *ACS Biomaterials Science & Engineering*
514 **4**:3522–3533. doi:10.1021/acsbiomaterials.8b00578

515 Bongomin F, Gago S, Oladele RO, Denning DW. 2017. Global and Multi-National
516 Prevalence of Fungal Diseases-Estimate Precision. *J Fungi (Basel)* **3**. doi:10.3390/jof3040057

517 Braissant O, Cailleau G, Aragno M, Verrecchia EP. 2004. Biologically induced
518 mineralization in the tree Milicia excelsa (Moraceae): its causes and consequences to the
519 environment. *Geobiology* **2**:59–66. doi:10.1111/j.1472-4677.2004.00019.x

520 Brown GD, Denning DW, Gow NAR, Levitz SM, Netea MG, White TC. 2012. Hidden
521 Killers: Human Fungal Infections. *Science Translational Medicine* **4**:165rv13.
522 doi:10.1126/scitranslmed.3004404

523 Brunke S, Mogavero S, Kasper L, Hube B. 2016. Virulence factors in fungal pathogens of
524 man. *Curr Opin Microbiol* **32**:89–95. doi:10.1016/j.mib.2016.05.010

525 Buffie CG, Bucci V, Stein RR, McKenney PT, Ling L, Gobourne A, No D, Liu H, Kinnebrew
526 M, Viale A, Littmann E, van den Brink MRM, Jenq RR, Taur Y, Sander C, Cross JR,
527 Toussaint NC, Xavier JB, Pamer EG. 2015. Precision microbiome reconstitution restores bile
528 acid mediated resistance to Clostridium difficile. *Nature* **517**:205–208.
529 doi:10.1038/nature13828

530 Cameselle C, Bohlmann JT, Núñez MJ, Lema JM. 1998. Oxalic acid production by
531 Aspergillus niger. *Bioprocess Engineering* **19**:247–252. doi:10.1007/pl00009017

532 Certini G, Corti G, Ugolini FC. 2000. Vertical trends of oxalate concentration in two soils

533 under Abies alba from Tuscany (Italy). *Journal of Plant Nutrition and Soil Science* **163**:173–
534 177. doi:10.1002/(SICI)1522-2624(200004)163:2<173::AID-JPLN173>3.0.CO;2-H

535 Charlson ES, Bittinger K, Haas AR, Fitzgerald AS, Frank I, Yadav A, Bushman FD, Collman
536 RG. 2011. Topographical Continuity of Bacterial Populations in the Healthy Human
537 Respiratory Tract. *American Journal of Respiratory and Critical Care Medicine* **184**:957–
538 963. doi:10.1164/rccm.201104-0655OC

539 Charlson ES, Diamond JM, Bittinger K, Fitzgerald AS, Yadav A, Haas AR, Bushman FD,
540 Collman RG. 2012. Lung-enriched Organisms and Aberrant Bacterial and Fungal Respiratory
541 Microbiota after Lung Transplant. *American Journal of Respiratory and Critical Care*
542 *Medicine* **186**:536–545. doi:10.1164/rccm.201204-0693OC

543 Cui L, Lucht L, Tipton L, Rogers MB, Fitch A, Kessinger C, Camp D, Kingsley L, Leo N,
544 Greenblatt RM, Fong S, Stone S, Dermand JC, Kleerup EC, Huang L, Morris A, Ghedin E.
545 2015. Topographic Diversity of the Respiratory Tract Mycobiome and Alteration in HIV and
546 Lung Disease. *American Journal of Respiratory and Critical Care Medicine* **191**:932–942.
547 doi:10.1164/rccm.201409-1583OC

548 de Oliveira Ceita G, Macêdo JNA, Santos TB, Alemanno L, da Silva Gesteira A, Micheli F,
549 Mariano AC, Gramacho KP, da Costa Silva D, Meinhardt L, Mazzafera P, Pereira GAG, de
550 Mattos Cascardo JC. 2007. Involvement of calcium oxalate degradation during programmed
551 cell death in Theobroma cacao tissues triggered by the hemibiotrophic fungus Moniliophthora
552 perniciosa. *Plant Science* **173**:106–117. doi:10.1016/j.plantsci.2007.04.006

553 Diamantstein T, Odenwald MV. 1974. Control of the immune response in vitro by calcium
554 ions. I. The antagonistic action of calcium ions on cell proliferation and on cell
555 differentiation. *Immunology* **27**:531–541.

556 Diamantstein T, Ulmer A. 1975. The control of immune response in vitro by Ca2+. II. The

557 Ca2+-dependent period during mitogenic stimulation. *Immunology* **28**:121–125.

558 Dickson RP, Martinez FJ, Huffnagle GB. 2014. The role of the microbiome in exacerbations
559 of chronic lung diseases. *The Lancet* **384**:691–702. doi:10.1016/S0140-6736(14)61136-3

560 Dominguez-Gutierrez PR, Kusmartsev S, Canales BK, Khan SR. 2018. Calcium Oxalate
561 Differentiates Human Monocytes Into Inflammatory M1 Macrophages. *Front Immunol*
562 **9**:1863. doi:10.3389/fimmu.2018.01863

563 Dutton MV, Evans CS. 1996. Oxalate production by fungi: its role in pathogenicity and
564 ecology in the soil environment. *Canadian Journal of Microbiology* **42**:881–895.
565 doi:10.1139/m96-114

566 Enaud R, Prevel R, Ciarlo E, Beaufils F, Wieërs G, Guery B, Delhaes L. 2020. The Gut-Lung
567 Axis in Health and Respiratory Diseases: A Place for Inter-Organ and Inter-Kingdom
568 Crosstalks. *Frontiers in Cellular and Infection Microbiology* **10**.
569 doi:10.3389/fcimb.2020.00009

570 Ferro KI. 2012. The impact of oxalogenic plants on soil carbon dynamics - formation of a
571 millennium carbon storage as calcium carbonate. *Faculty of Sciences*. Neuchâtel: University
572 of Neuchâtel.

573 Fisher MC, Gurr SJ, Cuomo CA, Blehert DS, Jin H, Stukenbrock EH, Stajich JE, Kahmann
574 R, Boone C, Denning DW, Gow NAR, Klein BS, Kronstad JW, Sheppard DC, Taylor JW,
575 Wright GD, Heitman J, Casadevall A, Cowen LE. 2020. Threats Posed by the Fungal
576 Kingdom to Humans, Wildlife, and Agriculture. *mBio* **11**. doi:10.1128/mBio.00449-20

577 Fisher MC, Hawkins NJ, Sanglard D, Gurr SJ. 2018. Worldwide emergence of resistance to
578 antifungal drugs challenges human health and food security. *Science* **360**:739–742.
579 doi:10.1126/science.aap7999

580 Foesel BU, Pfeiffer S, Raj ACD, Etschmann SK, Schloter M. 2019. Applying ecological
581 theories in lung microbiome research: lessons learned from microbial ecology and evolution?
582 In: Cox MJ, Ege MJ, von Mutius E, editors. The Lung Microbiome. pp. 50–66.
583 doi:10.1183/2312508x.10015718

584 Fulcher ML, Gabriel S, Burns KA, Yankaskas JR, Randell SH. 2005. Well-Differentiated
585 Human Airway Epithelial Cell Cultures In: Picot J, editor. Methods in Molecular Medicine.

586 Graustein WC, Cromack K Jr, Sollins P. 1977. Calcium oxalate: occurrence in soils and effect
587 on nutrient and geochemical cycles. *Science (Washington, DC)* 1252–1254.

588 Grinstein S, Klip A. 1989. Calcium homeostasis and the activation of calcium channels in
589 cells of the immune system. *Bull N Y Acad Med* **65**:69–79.

590 Hofmann BA, Bernasconi SM. 1998. Review of occurrences and carbon isotope geochemistry
591 of oxalate minerals: implications for the origin and fate of oxalate in diagenetic and
592 hydrothermal fluids. *Chemical Geology* **149**:127–146. doi:10.1016/S0009-2541(98)00043-6

593 Hsieh H-L, Nath P, Huang J-H. 2019. Multistep Fluidic Control Network toward the
594 Automated Generation of Organ-on-a-Chip. *ACS Biomaterials Science & Engineering*
595 **5**:4852–4860. doi:10.1021/acsbiomaterials.9b00912

596 Kousha M, Tadi R, Soubani AO. 2011. Pulmonary aspergillosis: a clinical review. *European*
597 *Respiratory Review* **20**:156–174. doi:10.1183/09059180.00001011

598 Kurrein F, Green GH, Rowles SL. 1975. Localized Deposition of Calcium Oxalate around a
599 Pulmonary Aspergillus niger Fungus Ball. *American Journal of Clinical Pathology* **64**:556–
600 563. doi:10.1093/ajcp/64.4.556

601 Lawley TD, Clare S, Walker AW, Stares MD, Connor TR, Raisen C, Goulding D, Rad R,
602 Schreiber F, Brandt C, Deakin LJ, Pickard DJ, Duncan SH, Flint HJ, Clark TG, Parkhill J,

603 Dougan G. 2012. Targeted Restoration of the Intestinal Microbiota with a Simple, Defined
604 Bacteriotherapy Resolves Relapsing Clostridium difficile Disease in Mice. *PLoS Pathog*
605 **8**:e1002995. doi:10.1371/journal.ppat.1002995

606 Lehner A, Meimoun P, Errakhi R, Madiona K, Barakate M, Bouteau F. 2008. Toxic and
607 signalling effects of oxalic acid. *Canadian Journal of Microbiology* **3**:746–748.
608 doi:10.1093/jxb/ern166.746

609 Lin CK, Hsiao YY, Nath P, Huang JH. 2019. Aerosol delivery into small anatomical airway
610 model through spontaneous engineered breathing. *Biomicrofluidics* **13**:044109.
611 doi:10.1063/1.5121188

612 Maeno T, Sasaki M, Shibue Y, Mimura K, Oka H. 2015. Calcium oxalate in the sputum may
613 aid in the diagnosis of pulmonary aspergillosis: A report of two cases. *Med Mycol Case Rep*
614 **8**:32–6. doi:10.1016/j.mmcr.2015.01.003

615 Martin G, Guggiari M, Bravo D, Zopfi J, Cailleau G, Aragno M, Job D, Verrecchia E, Junier
616 P. 2012. Fungi, bacteria and soil pH: The oxalate-carbonate pathway as a model for metabolic
617 interaction. *Environmental Microbiology* **14**:2960–2970. doi:10.1111/j.1462-
618 2920.2012.02862.x

619 McClintock SD, Attili D, Dame MK, Richter A, Silvestri SS, Berner MM, Bohm MS,
620 Karpoff K, McCarthy CL, Spence JR, Varani J, Aslam MN. 2020. Differentiation of human
621 colon tissue in culture: Effects of calcium on trans-epithelial electrical resistance and tissue
622 cohesive properties. *PLoS ONE* **15**:e0222058. doi:10.1371/journal.pone.0222058

623 Mela F, Fritsche K, de Boer W, van Veen JA, de Graaff LH, van den Berg M, Leveau JH.
624 2011. Dual transcriptional profiling of a bacterial/fungal confrontation: Collimonas
625 fungivorans versus Aspergillus niger. *ISME J* **5**:1494–504. doi:10.1038/ismej.2011.29

626 Miller A, Dearing D. 2013. The Metabolic and Ecological Interactions of Oxalate-Degrading
627 Bacteria in the Mammalian Gut. *Pathogens* **2**:636–652. doi:10.3390/pathogens2040636

628 Mitchell AB, Oliver BGG, Glanville AR. 2016. Translational Aspects of the Human
629 Respiratory Virome. *American Journal of Respiratory and Critical Care Medicine* **194**:1458–
630 1464. doi:10.1164/rccm.201606-1278CI

631 Mulay SR, Kulkarni OP, Rupanagudi KV, Migliorini A, Darisipudi MN, Vilaysane A,
632 Muruve D, Shi Y, Munro F, Liapis H, Anders HJ. 2013. Calcium oxalate crystals induce renal
633 inflammation by NLRP3-mediated IL-1beta secretion. *J Clin Invest* **123**:236–46.
634 doi:10.1172/JCI63679

635 Muntz FH. 1999. Oxalate-producing pulmonary aspergillosis in an alpaca. *Vet Pathol*
636 **36**:631–2. doi:10.1354/vp.36-6-631

637 Oda M, Saraya T, Wakayama M, Shibuya K, Ogawa Y, Inui T, Yokoyama E, Inoue M,
638 Shimoyamada H, Fujiwara M, Ota T, Takizawa H, Goto H. 2013. Calcium oxalate crystal
639 deposition in a patient with Aspergilloma due to Aspergillus niger. *J Thorac Dis* **5**:E174-8.
640 doi:10.3978/j.issn.2072-1439.2013.08.45

641 Pabuççuoğlu U. 2005. Aspects of oxalosis associated with aspergillosis in pathology
642 specimens. *Pathology Research and Practice* **201**:363–368. doi:10.1016/j.prp.2005.03.005

643 Palmieri F, Estoppey A, House GL, Lohberger A, Bindschedler S, Chain PSG, Junier P. 2019.
644 Oxalic acid, a molecule at the crossroads of bacterial-fungal interactions. *Adv Appl Microbiol*
645 **106**:49–77. doi:10.1016/bs.aambs.2018.10.001

646 Paulussen C, Hallsworth JE, Alvarez-Perez S, Nierman WC, Hamill PG, Blain D, Rediers H,
647 Lievens B. 2017. Ecology of aspergillosis: insights into the pathogenic potency of Aspergillus
648 fumigatus and some other Aspergillus species. *Microb Biotechnol* **10**:296–322.

649 doi:10.1111/1751-7915.12367

650 Payne CL, Dark MJ, Conway JA, Farina LL. 2017. A retrospective study of the prevalence of
651 calcium oxalate crystals in veterinary Aspergillus cases. *J Vet Diagn Invest* **29**:51–58.
652 doi:10.1177/1040638716672254

653 Pfaller MA, Diekema DJ. 2004. Rare and Emerging Opportunistic Fungal Pathogens:
654 Concern for Resistance beyond Candida albicans and Aspergillus fumigatus. *Journal of*
655 *Clinical Microbiology* **42**:4419–4431. doi:10.1128/jcm.42.10.4419-4431.2004

656 Ramirez-Ortiz ZG, Means TK. 2012. The role of dendritic cells in the innate recognition of
657 pathogenic fungi (A. fumigatus, C. neoformans and C. albicans). *Virulence* **3**:635–46.
658 doi:10.4161/viru.22295

659 Reasoner DJ, Geldreich EE. 1985. A new medium for the enumeration and subculture of
660 bacteria from potable water. *Applied and Environmental Microbiology* **49**:1.

661 Ruijter GJG, van de Vondervoort PJI, Visser J. 1999. Oxalic acid production by Aspergillus
662 niger: an oxalate-non-producing mutant produces citric acid at pH 5 and in the presence of
663 manganese. *Microbiology* **145**:2569–2576. doi:10.1099/00221287-145-9-2569

664 Şahin N, Işik K, Tamer AÜ, Goodfellow M. 2000. Taxonomic Position of "Pseudomonas
665 oxalaticus" Strain Ox1T (DSM 1105T) (Khambata and Bhat, 1953) and its Description in the
666 Genus Ralstonia as Ralstonia oxalatica comb. nov. *Systematic and Applied Microbiology*
667 **23**:206–209. doi:10.1016/s0723-2020(00)80006-5

668 Sentchilo V, Czechowska K, Pradervand N, Minoia M, Miyazaki R, van der Meer JR. 2009.
669 Intracellular excision and reintegration dynamics of the ICEclc genomic island of
670 Pseudomonas knackmussii sp. strain B13. *Mol Microbiol* **72**:1293–306. doi:10.1111/j.1365-
671 2958.2009.06726.x

672 Suleyman G, Alangaden GJ. 2016. Nosocomial Fungal Infections: Epidemiology, Infection
673 Control, and Prevention. *Infect Dis Clin North Am* **30**:1023–1052.
674 doi:10.1016/j.idc.2016.07.008

675 Suryavanshi MV, Bhute SS, Jadhav SD, Bhatia MS, Gune RP, Shouche YS. 2016.
676 Hyperoxaluria leads to dysbiosis and drives selective enrichment of oxalate metabolizing
677 bacterial species in recurrent kidney stone endures. *Scientific Reports* **6**.
678 doi:10.1038/srep34712

679 Ticinesi A, Nouvenne A, Chiussi G, Castaldo G, Guerra A, Meschi T. 2020. Calcium Oxalate
680 Nephrolithiasis and Gut Microbiota: Not just a Gut-Kidney Axis. A Nutritional Perspective.
681 *Nutrients* **12**. doi:10.3390/nu12020548

682 Toprak E, Veres A, Michel JB, Chait R, Hartl DL, Kishony R. 2011. Evolutionary paths to
683 antibiotic resistance under dynamically sustained drug selection. *Nat Genet* **44**:101–5.
684 doi:10.1038/ng.1034

685 Turroni S, Vitali B, Bendazzoli C, Candela M, Gotti R, Federici F, Pirovano F, Brigidi P.
686 2007. Oxalate consumption by lactobacilli: Evaluation of oxalyl-CoA decarboxylase and
687 formyl-CoA transferase activity in Lactobacillus acidophilus. *Journal of Applied*
688 *Microbiology* **103**:1600–1609. doi:10.1111/j.1365-2672.2007.03388.x

689 van Woerden HC, Gregory C, Brown R, Marchesi JR, Hoogendoorn B, Matthews IP. 2013.
690 Differences in fungi present in induced sputum samples from asthma patients and non-atopic
691 controls: a community based case control study. *BMC Infectious Diseases* **13**:69.
692 doi:10.1186/1471-2334-13-69

693 Vig M, Kinet J-P. 2009. Calcium signaling in immune cells. *Nature Immunology* **10**:21–27.
694 doi:10.1038/ni.f.220

695 Yi Y, Cho SY, Lee DG, Jung JI, Park YJ, Lee KY. 2019. Invasive Pulmonary Aspergillosis
696 Due to Aspergillus awamori: Role of Calcium Oxalate Crystal Precipitation Mimicking
697 Mucormycosis. *Mycopathologia*. doi:10.1007/s11046-019-00405-z

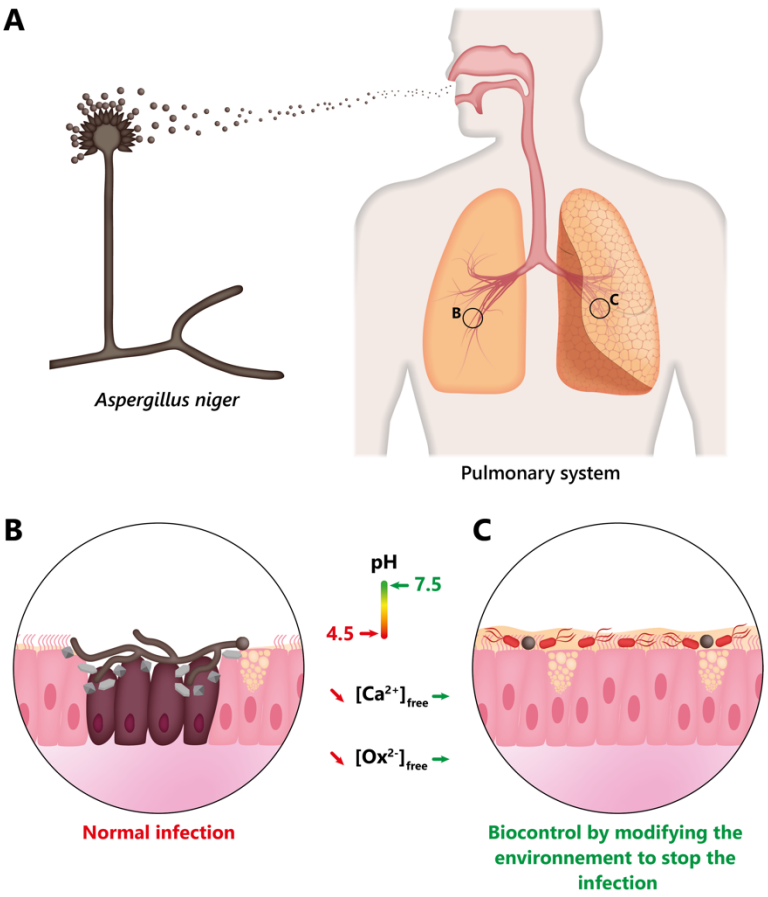

Fig. 1. Schematic summary of the proposed strategy to control *Aspergillus niger* infection by introducing oxalotrophic bacteria to modify the *A. niger* environmental niche. (A) *A. niger* conidia (depicted in dark grey) arrive in the respiratory system through breathing. (B) During a normal infection process in a susceptible host, *A. niger* modifies the environment by secreting oxalic acid (or oxalate Ox^{2-}) which decreases pH and chelates free calcium in the form of calcium oxalate (CaOx; depicted in light grey) crystals. This results in the infection of the host's tissue. (C) The biocontrol strategy proposed here takes advantage of the ability of oxalotrophic bacteria (cells depicted in red) to consume CaOx and thus reestablish physiological pH and free calcium concentrations.

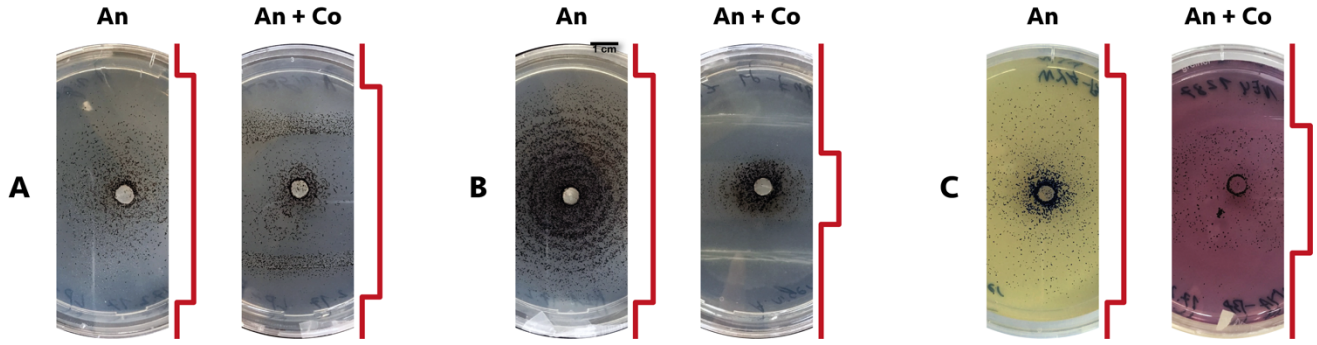

Fig. 2. Comparison of the growth of *Aspergillus niger* (An) alone and in confrontation with *Cupriavidus oxalaticus* (Co) in different culture media. The red line next to each picture represents the extent of *A. niger* growth. On MA 1/10 (A), there is no significant growth inhibition of *A. niger*, as it kills *C. oxalaticus*. *A. niger* growth is highly restricted to the center of the plate when co-cultured with *C. oxalaticus* on R2A (B). The growth inhibition of *A. niger* when co-cultured with *C. oxalaticus* is less pronounced on WYA + BP (C).

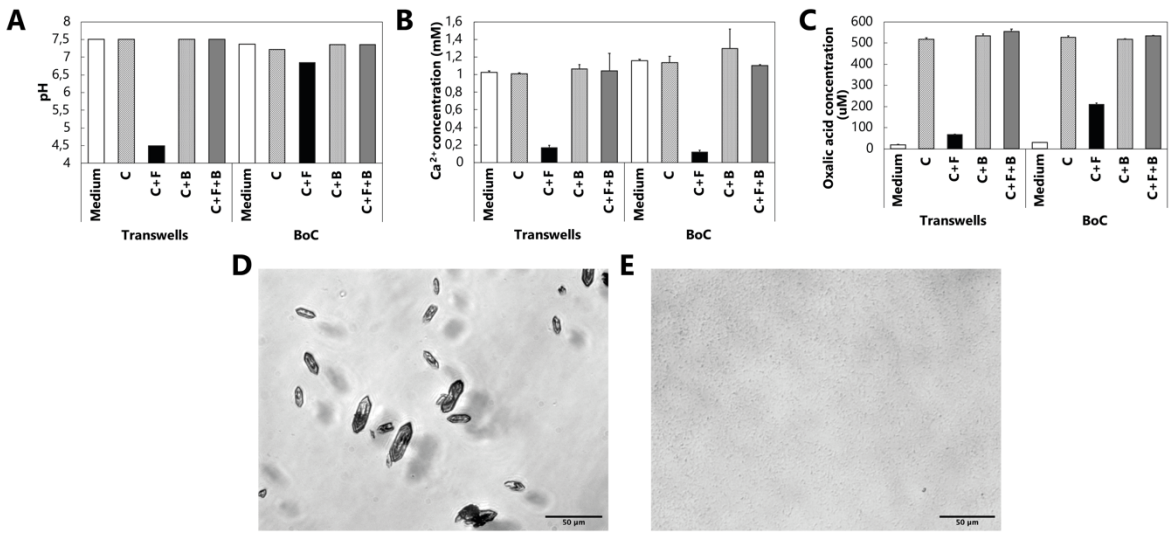

Fig. 3. Influence of the interaction between *Aspergillus niger* and the oxalotrophic bacterium *Cupriavidus oxalaticus* on environmental parameters of differentiated bronchial tissue in Transwell® inserts and bronchiole-on-a-chip (BoC) devices. In the presence of the fungus, the pH (A) decreases, as compared to all other treatments. This pH decrease is correlated with a drastic decrease in the concentration of free Ca^{2+} (B) (*p*-value between C and C+F = $8{,}951 \times 10^{-7}$**)**. Free oxalic acid concentrations were lower in the presence of the fungus, compared with the basal level secreted by the bronchial cells (C) (*p*-value between C and C+F = $4{,}587 \times 10^{-8}$**)**. These results are supported by the detection of calcium oxalate crystals in the presence of the fungus (D). In the co-culture with the oxalotrophic bacterium, pH, free Ca^{2+} and free oxalic acid concentrations return to physiological levels, and this was concomitant with the absence of crystals (E) (*p*-values between C+F and C+F+B for free Ca^{2+} and free oxalic acid = 0,002 and $1{,}415 \times 10^{-7}$, respectively). C: lung cells; C+F: lung cells + fungus; C+B: lung cells + bacteria; C+F+B: lung cells + fungus + bacteria. For A, B, C, the results represent the mean + sd of three independent measurements for the Transwell® inserts for each condition (three biological replicates, n = 3). For A, pH results for the BoC devices represent a unique measurement per condition (one replicate, n = 1). For B and C, Ca^{2+}

734 and oxalic acid results for the BoC devices represents the mean + sd of two measurements per

735 condition (one replicate).

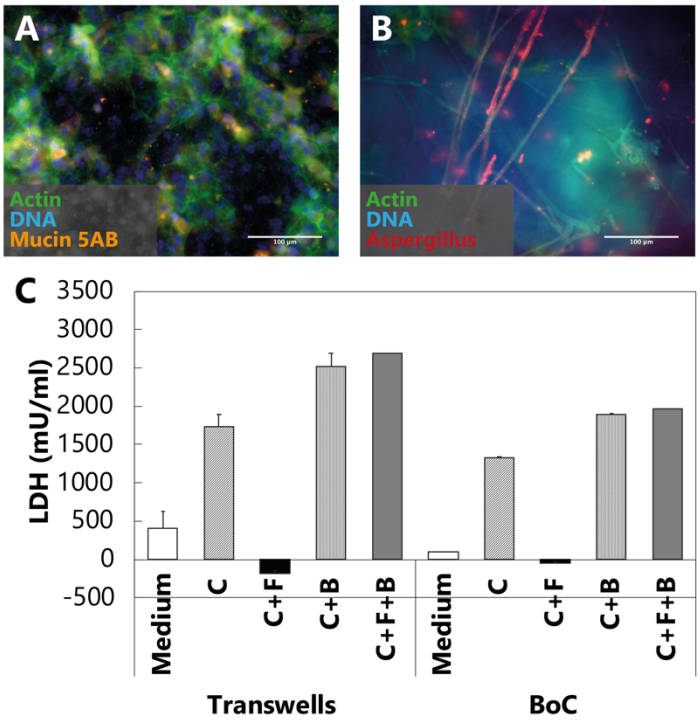

736

737 **Fig. 4. Cytopathic effect of *Aspergillus niger* on differentiated bronchial tissue and lactate**
738 **dehydrogenase (LDH) measurements of the co-culture between *A. niger* and *Cupriavidus***
739 ***oxalaticus* in Transwell® inserts and bronchiole-on-a-chip (BoC) devices.** (A) Control
740 showing healthy differentiated bronchial epithelial cells. (B) Bronchial epithelial cells infected
741 with *A. niger*. (C) LDH leakage was measured as a proxy for cell damage. In the presence of
742 the fungus, no LDH has been detected, probably because of the destruction of the tissue by *A.*
743 *niger* (B). *C. oxalaticus* cause significantly more LDH leakage that the basal LDH level of
744 control cells (p-value = 0,004). C: lung cells; C+F: lung cells + fungus; C+B: lung cells +
745 bacteria; C+F+B: lung cells + fungus + bacteria. For C, the results represent the mean + sd of
746 three independent measurements for the Transwell® inserts for each condition (three biological
747 replicates, n = 3). LDH results for the BoC devices represents the mean + sd of three
748 measurements per condition (one replicate, n = 1).